catalysts

MDPI

Article

Photocatalysis: A Possible Vital Contributor to the Evolution of the Prebiotic Atmosphere and the Warming of the Early Earth

Chuchu Cheng †, Fangjie Xu †, Wenwen Shi, Qiaoyun Wang and Caijin Huang *

State Key Laboratory of Photocatalysis on Energy and Environment, College of Chemistry, Fuzhou University, Fuzhou 350116, China; cccheng@dicp.ac.cn (C.C.); 211320199@fzu.edu.cn (F.X.); 211320204@fzu.edu.cn (W.S.); 221310057@fzu.edu.cn (Q.W.)

* Correspondence: cjhuang@fzu.edu.cn

† These authors contributed equally to this work.

Abstract: The evolution of the early atmosphere was driven by changes in its chemical composition, which involved the formation of some critical gases. In this study, we demonstrate that nitrous oxide (N_2O) can be produced from Miller's early atmosphere (a mixture of CH_4, NH_3, H_2, and H_2O) by way of photocatalysis. Both NH_3 and H_2O were indispensable for the production of N_2O by photocatalysis. Different conditions related to seawater and reaction temperature are also explored. N_2O has a strong greenhouse gas effect, which is more able to warm the Earth than other gases and offers a reasonable explanation for the faint young Sun paradox on the early Earth. Moreover, the decomposition of N_2O into N_2 and O_2 can be boosted by soft irradiation, providing a possible and important origin of atmospheric O_2 and N_2. The occurrence of O_2 propelled the evolution of the atmosphere from being fundamentally reducing to oxidizing. This work describes a possible vital contribution of photocatalysis to the evolution of the early atmosphere.

Keywords: origin of O_2; nitrous oxide; faint young sun paradox; photocatalysis; early earth

Citation: Cheng, C.; Xu, F.; Shi, W.; Wang, Q.; Huang, C. Photocatalysis: A Possible Vital Contributor to the Evolution of the Prebiotic Atmosphere and the Warming of the Early Earth. *Catalysts* **2023**, *13*, 1310. https://doi.org/10.3390/catal13091310

Academic Editors: Weilong Shi, Feng Guo, Xue Lin and Yuanzhi Hong

Received: 14 August 2023
Revised: 17 September 2023
Accepted: 18 September 2023
Published: 20 September 2023

1. Introduction

The Earth experienced a fainter Sun in its early stages. In the ancient Archean eon, the early Earth received only 76–83% of the energy from the Sun that it does today [1]. As a consequence, the Earth would have become covered with ice if the greenhouse effect and surface albedo were the same as in the present. However, geological evidence has uncovered the presence of liquid H_2O on the early Earth's surface, and the Archean may have been warmer than today, as we are currently in a period of glaciation [2,3]. This is known as "the faint young Sun paradox" [4,5]. To date, many hypotheses have been proposed to resolve this paradox, but there is still no clear conclusion at present.

The chemical composition change of the Earth's early atmosphere played a vital role in the atmospheric evolution, climate change, and the evolution of the early Earth to the modern Earth suited for life. For instance, a high concentration of greenhouse gases (CH_4 and CO_2) has been suggested to help to resolve "the faint young Sun paradox". However, geological evidence has demonstrated that the concentration of these two greenhouse gases in the early atmosphere could not have been high enough to satisfy this paradox [6]. Alternatively, Airapetian et al. proposed that the energetic particles from an active young Sun penetrated the atmosphere and converted N_2, CH_4, and CO_2 to N_2O and hydrogen cyanide (HCN) [7]. It has been found that the greenhouse effect of N_2O (298 GWP) is much stronger than those of CH_4 (82.5 GWP) and CO_2 (1 GWP) [8,9], which means that N_2O has a much stronger greenhouse effect, and has more potential to have warmed the early Earth. Moreover, Nna-Mvondo et al. found that oxynitride (NO and N_2O) can be produced in a mimetic Hadean and Archean atmosphere (CO_2-N_2 mixture) by lightning and coronal discharge [10]. Nevertheless, low oxynitride yield by this means and light-induced decomposition would have limited N_2O accumulation on the early Earth. Therefore, there

is possibly an overlooked process for the stable and abiotic mass production of N_2O, which may be key to explaining "the faint young Sun paradox".

In addition to the Earth's early temperature, the origin of O_2 is another mystery of the evolution of the atmosphere. It has been proven that the O_2 level of the early Earth changed substantially over geological time [11]. For example, molybdenum isotopes found in the rocks of South Africa indicate the possible emergence of substantial free O_2 in shallow marine environments approximately 3 Gyr [12]. Some models have demonstrated that "O_2 oases" may have been created before the Great Oxidation Event (GOE) [13,14]. The origins and rise of atmospheric O_2 on the early Earth have aroused wide interest. O_2-producing cyanobacteria or other green non-sulfur bacteria are considered to have promoted the evolution of the early Earth's atmosphere to an O_2-rich atmosphere [15]. The recent results of CO_2 photodissociation experiments may have implications for non-biological O_2 production in a CO_2-heavy atmosphere [16,17]. Since N_2O can be decomposed into O_2 and N_2 through thermocatalysis or under soft irradiation [18,19], atmospheric O_2 could be related to the level of N_2O if the large-scale generation of N_2O was possible on the early Earth. Moreover, some studies have also reported the decomposition of N_2O into O_2 and N_2 from the perspective of photodissociation dynamics [20,21].

Different sources of energy, such as ultraviolet light, electrical discharges, radioactivity, and volcanoes, have been examined in many experimental studies on prebiotic chemistry [22]. Among these energy sources, solar energy is the most powerful and continuous source of energy. Photocatalysis can use abundant solar energy to achieve solar-to-chemical energy conversion, and has attracted widespread research interest in recent decades [23–25]. Additionally, the radiation level on the early Earth was several orders of magnitude higher in the short wavelength range than the current level at the Earth's surface [26,27]. It could be assumed that semiconductor minerals turned the surface of the early Earth into a photoreactor under the conditions of high ultraviolet irradiation and the early Earth's thin atmosphere [28]. Interestingly, Harald et al. obtained a mixture of amino acids from an NH_3 solution with CH_4 over a Pt/TiO_2 photocatalyst under irradiation from an Xe lamp [29]. Although great efforts have been made to account for the evolution of the early Earth and the origin of O_2, few hypotheses have focused on the contribution of photocatalysis which may have played an important role in these processes [30,31].

In this work, we present a feasible photocatalytic way to efficiently produce N_2O from a mimicked early reducing atmosphere using natural semiconductor materials (i.e., TiO_2) under light irradiation. TiO_2, one of the most widely used and chemically stable photocatalysts, is abundant on Earth, as well as on other planets such as Mars [32]. Herein, we used TiO_2 for the photocatalytic conversion of the mimicked early reducing atmosphere (CH_4, H_2, H_2O, and NH_3) applied in Miller's experiments. The photocatalytic oxidation of NH_3 to N_2O may be a feasible and important way to understand the chemical evolution of the early Earth. Since N_2O has a strong greenhouse effect, the steady generation of N_2O could have caused a warm early Earth, and the decomposition of N_2O by solar light may have produced abiogenic O_2 for the early Earth. Furthermore, we attempt here to explain the two primary enigmas (the faint young Sun paradox and the origin of atmospheric O_2) of the early Earth.

2. Results and Discussion

2.1. The Faint Young Sun Paradox

A mixture of gases (CH_4, H_2, H_2O, and NH_3), similar to that used in Miller's experiment, was employed to mimic the early reducing atmosphere. Among these gases, NH_3 is considered a probable part of the composition of the early atmosphere [33–35], which may come from the degasification of the Earth or have been generated from nitrate through denitrification [34,36,37]. It has been noted that the ammonium concentration of Paleoarchean metasedimentary biotite grains reached up to several hundred ppm [38], which raises the possibility of a NH_3-rich atmosphere on the early Earth. Nitrogen isotope ratios have offered evidence for the existence of the oldest known alkaline lake system which may

have provided alkaline conditions for the volatilization of NH_3 gas [39]. Therefore, NH_3 may have been a sufficient reactant for the production of N_2O on the early Earth.

Solar light is continuous and had high ultraviolet irradiance on the early Earth, which allows it to meet the needs of photocatalytic reactions [27,40]. If N_2O can be effectively produced from the primitive atmosphere (including NH_3 and H_2O) with inexhaustible solar energy, a possible explanation could be offered to address the faint young Sun paradox. N_2O is generally considered to primarily enter the atmosphere as a byproduct of biological nitrification and denitrification [33,41]; oceanic O_2 restricted the concentration of N_2O on the early Earth [42] because N_2O is rapidly photodissociated at lower atmospheric O_2 levels. In this work, we present experimental evidence that N_2O can be generated from and accumulated in a mimicked early reducing and anoxic atmosphere (NH_3, H_2O) via photocatalysis. Thus, the concentration of N_2O need not be dependent on O_2 levels or biological enzymes.

For the simplification and reliability of the reaction system, commercial TiO_2 powder was chosen instead of natural semiconducting minerals due to the lower symmetries and additional complexities of the latter. The commercial TiO_2 powder was evaluated using X-ray diffraction (XRD), high-resolution transmission electron microscopy (HRTEM), diffusion reflectance spectroscopy (DRS), and X-ray photoelectron spectroscopy (XPS) (Figures S1 and S2). The crystal phase of the applied TiO_2 was anatase, and its average particle size was approximately 5 nm. Our experiment was performed in an airtight silica tube (Figure 1) containing mixed gases, water, and photocatalyst. The mixed gases mimic the primitive atmosphere (CH_4, H_2, and NH_3), as used in Miller's experiments [43], and the aqueous solution represents the primitive ocean. The gas composition was monitored using a Fourier transform infrared spectrometer (FTIR) through the CaF_2 window. After 5 days of photocatalytic reaction, obvious double peaks were observed at around 2238 and 2213 cm^{-1}, corresponding to N_2O [44] (Figure 2a). The generation of N_2O indicated that both NH_3 and H_2O were indispensable for the reaction; thus, we used NH_3 and H_2O as reactants in the subsequent experiments. As expected, N_2O was can be also produced (Figure 2b), and the amount of N_2O gradually increased day by day via photocatalytic reaction (Figure 3a) with the photocatalyst and light illumination. In this reaction, NH_3 is oxidized to N_2O and water is reduced to H_2 ($2NH_3 + H_2O \rightarrow N_2O + 4H_2$). The amount of H_2 is shown in Figure S3. Additionally, we detected the concentration of NO_3^- and NO_2^- in the liquid phase (Figure S4) and no obvious signal was observed, which indicates N_2O is the single oxidative product of NH_3. Meanwhile, even when the reaction temperature was adjusted to 3 °C, the formation of N_2O still proceeded (Figure 2c) (note that negative double peaks around 2348 cm^{-1} are attributed to the fluctuation of CO_2 concentration in the air (outside the reaction tube), which did not influence the reaction). Furthermore, we also investigated simulated present-day seawater (0.462 M NaCl, 1.3 mM $MgSO_4$, 0.04 M $MgCl_2$, and 6.8 mM $MgBr_2$) instead of pure water for photocatalytic N_2O production. After 7 days of irradiation, obvious double peaks were observed at around 2238 and 2213 cm^{-1}, corresponding to N_2O (Figure 2d) with no new peaks observed. Moreover, the amount of N_2O evolution was further detected using gas chromatography [45] (Figure 3b). The highest evolution rate of N_2O was measured at approximately 20 μmol per day. For comparison, in the absence of a catalyst or light irradiation, the target product (N_2O) was nearly undetectable in the control experiments (Figure 4).

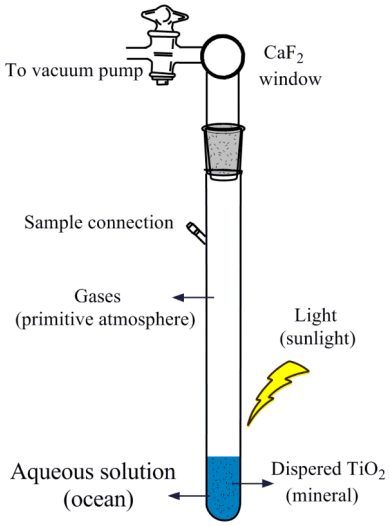

Figure 1. Schematic drawing of the experimental apparatus.

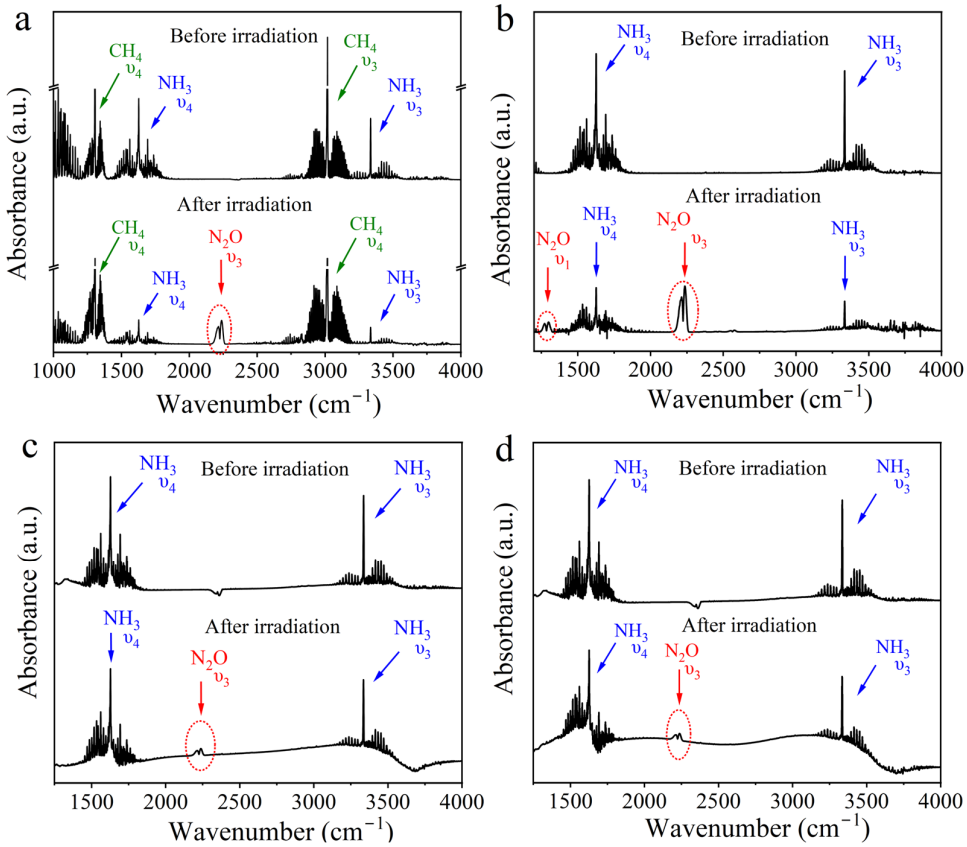

Figure 2. FTIR spectra of gas phase before irradiation and after 5 days of irradiation. Reaction gas: (**a**) CH_4, H_2, H_2O, and NH_3; (**b**) reaction gas: NH_3 and H_2O; reaction conditions: 10 mL H_2O, ambient temperature; (**c**) reaction gas: NH_3 and H_2O; reaction conditions: 10 mL H_2O, 3 °C; (**d**) reaction gas: NH_3 and H_2O; reaction conditions: 10 mL simulated seawater, ambient temperature.

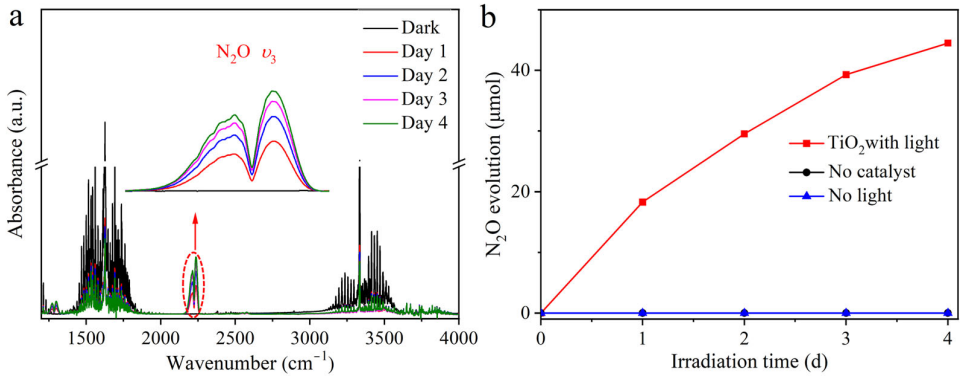

Figure 3. The evolution of N_2O via photocatalytic oxidation of NH_3. (**a**) FTIR spectra of gas phase over 4 days of reaction; (**b**) the evolution rate of N_2O with TiO_2 with light (red line), without any catalyst (black line), and without light (blue line).

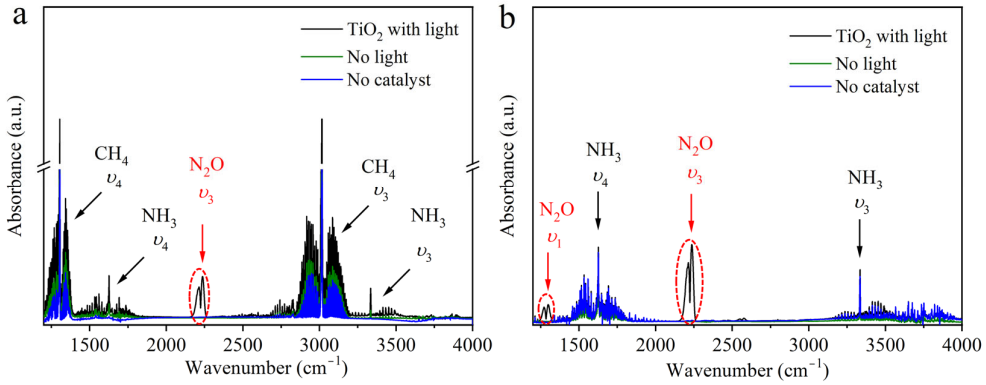

Figure 4. Spectra of the gas-phase mixture after 5 days of reaction with titanium dioxide and light (black line), without light (green line), and without any catalyst (blue line) [44]. Reactant gas: (**a**) CH_4, H_2, H_2O, and NH_3; (**b**) NH_3 and H_2O.

Owing to the limited gas tightness and vacuum degree of the experimental apparatus, the effect of ambient O_2 could not be entirely excluded in our experiments. To verify that the oxygen atoms in N_2O originated from H_2O, ^{18}O-labeled H_2O was added into the reaction system. Table 1 shows the ratios of ^{18}O in ^{18}O-labeled H_2O and N_2O. The ^{18}O content of the generated N_2O reached 0.405 atom%, which was apparently higher than the natural abundance (0.2 atom%). This proves the feasible transfer of oxygen atom from H_2O to N_2O, and approximately 16% of the N_2O in our system was from the reduction of H_2O due to the competition of ambient O_2.

Table 1. Oxygen isotopic compositions of N_2O and ^{18}O-labeled H_2O.

Sample	Ampl 44/28	$\delta^{18}O_{V\text{-}SMOW}$‰	AT% $^{18}O/^{16}O$
^{18}O-labeled H_2O	486	7209.5	1.4826
N_2O	126	1018.3	0.4051

To estimate N_2O production by photocatalysis on the early Earth, we assumed that the irradiated surface area was equal to the internal cross-section of the tube (8 cm^2); therefore, the reaction rate on the irradiated surface area was 25 $mmol/m^2/day$. Given that the land area of the early Earth was similar to that of the modern Earth (149 million square kilometers) and that the proportion of TiO_2 area was approximately 1% according to the geochemical data of the modern Earth and terrestrial planets [46,47], the rate of production of N_2O by photoreduction was approximately 4×10^{11} g yr^{-1} (grams per year), which

was much larger than that predicted using the discharge method (9×10^7 g yr^{-1}) [10]. Additionally, we also carried out a gas–solid photocatalytic reaction experiment in which TiO_2 powder was deposited on a glass substrate placed above the surface of the water. The reaction rate on the irradiated surface area was 10 mmol/m^2/day (Figure 5) and the corresponding estimated production of N_2O was, thus, approximately 2×10^{11} g yr^{-1}, which is a potential origin of greenhouse gas able to offset reduced insolation in the early Earth and maintain a warm climate. Additionally, since N_2O has a stronger greenhouse effect than CH_4 or CO_2 [48], a lower N_2O concentration would have been needed to warm the early Earth. Crucially, the removal of N_2O from the atmosphere is much lower than that of CH_4, given that the steady-state lifetime of N_2O is approximately 120 years. Less than 1% of atmospheric N_2O is removed annually from the atmosphere, primarily by photolysis and oxidative reactions in the stratosphere [48]. Therefore, it is reasonable to assume that over geological time, with abundant energy sources and sufficient reactant, atmospheric N_2O may have created an insulating layer for the Earth, which may have helped to maintain liquid H_2O on the early Earth and stopped cosmic rays from reaching the Earth at the same time.

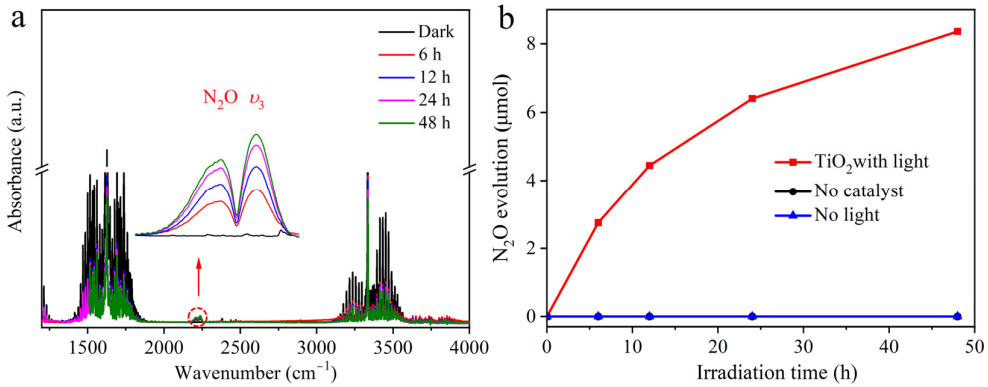

Figure 5. (**a**) FTIR spectra of the gas-phase mixture over 48 h of photocatalytic reaction. (**b**) The evolution rate of N_2O with TiO_2 and light (red line), and without any catalyst (black line), without light (blue line). Reaction conditions: 30 mg catalyst deposited on a glass substrate (2 cm × 2 cm), NH_3, 10 mL H_2O, ambient temperature.

2.2. The Possible Origin of Atmospheric O_2

Molecular oxygen has played an indispensable role in transforming our planetary environment. Its presence in the atmosphere and oceans has also induced planetary-scale interactions between the biosphere and the environment, leading to the Earth's system having crossed irreversible thresholds to reach its modern state. Rare earth element analyses of limestones and deep-water iron-rich sediments have shown that shallow water was oxygenated, whereas the adjacent deeper waters were not [14,49]. Regardless of the arguments raised by some studies that UV radiation would limit the expansion of cyanobacteria [50], the possible existence of "Archean cyanobacteria" could account for the oxygenation of shallow water [13,51,52]. The record of redox-sensitive trace-metals and C and S contents in black shales indicates that ocean ventilation on a global scale was delayed until later in the Cambrian with regard to rising oxygen levels in the atmosphere [53]. Notably, N_2O can be decomposed under solar light into O_2 and N_2 through thermocatalysis and photocatalysis [18,19,54], which may be an important origin of non-biological O_2 on the early Earth. Moreover, the photocatalytic generation and photodecomposition of N_2O can increase the O_2 level in shallow water but not in deep water, as deep water's lack of solar light cannot satisfy the conditions of photocatalytic reaction. This hypothesis posits that an increase in the oxygen content of shallow water was physiologically necessary for the emergence of large, highly energetic animals [55]. Although these findings are only preliminary, they still add evidence for the existence of N_2O and O_2.

Furthermore, it has been widely reported that the decomposition of N_2O gas to N_2 and O_2 can be induced by light. To our delight, previous studies have revealed the isotope fractionation of nitrogen atoms in the upper atmosphere and ascribed it to the ultraviolet (UV) photodissociation dynamics of N_2O. N_2O also has a broad absorption band that peaks at 182 nm, which means that it can absorb UV; the window of solar radiation occurs in the red wing of this band [56,57]. Moreover, the Gibbs free energy change (ΔG) of the decomposition of N_2O is −100 KJ, which means this reaction can react spontaneously. Based on these theories, we explored the decomposition of N_2O under solar light with TiO_2. To explore the significance of light and catalysis, we also removed TiO_2 and light during photocatalytic N_2O decomposition. Owing to the limited gas tightness and vacuum degree of the experiment apparatus, the effect of the surrounding O_2 could not be entirely rejected, so we only detected the concentrations of N_2O and N_2. Furthermore, before irradiation, we maintained the pressure of the tube at 1 bar to minimize gas exchange with the air outside the tube. As briefly shown in Figure 6a, the concentration of N_2O gradually decreased with the extension of illumination time, whereas the corresponding N_2 showed positive growth. To determine the effects of the photocatalyst and light, we carried out the N_2O decomposition experiment with the participation of TiO_2. As exhibited in Figure 6b, N_2O was smoothly decomposed into N_2 and O_2 with light, even without the assistance of TiO_2. However, it was difficult for N_2O to decompose in the dark because of the inhibitive high reaction energy of N_2O. Instead, the reaction energy decreased dramatically, contributing to the decomposition of N_2O in the presence of photoexcited or excess electrons on the TiO_2 surface. Simultaneously, we found that the evolution rate of N_2O with TiO_2 and light became slower after approximately 10 h of irradiation (Figures 3b and 5b). This indicates that the N_2O began to decompose when the concentration of N_2O reached a certain value, which is in agreement with our assumption of the decomposition of N_2O into O_2 and N_2.

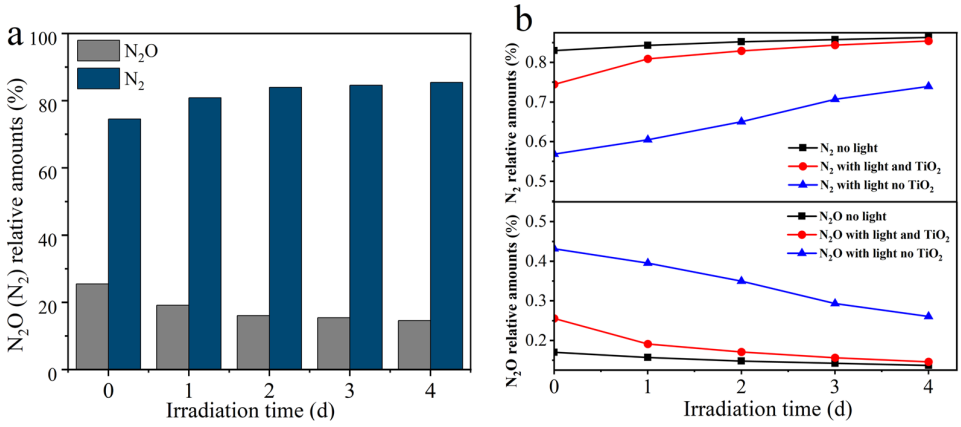

Figure 6. (**a**) Content of N_2O and N_2 mixture after several days of reaction with light and TiO_2; (**b**) comparison of the contents of N_2O and N_2 mixture after several days of reaction without light (black line), with light and TiO_2 (blue line), and with light but no TiO_2 (red line). "Relative amounts" refers to the gas proportion of N_2 or N_2O to the sum of N_2 and N_2O.

The physical and chemical properties of the reactants and photocatalyst can support our proposed model of nitrogen cycling. Firstly, ammonia in liquid water profoundly depresses the freezing point of the mixture. Some studies have also shown evidence of liquid water temperatures at the Earth's surface using the dating of sedimentary rocks which were laid down under water [52,58]. These conditions described by these theories could provide sufficient reactants (H_2O and NH_3) for the photocatalytic production of N_2O. Meanwhile, UV radiation would also provide a limitless energy source for the photocatalytic reaction without destroying the photocatalyst. Crucially, it is worth noting that throughout the production of N_2O, even after 30 h irradiation, the TiO_2 still exhibited perfect photocatalytic activity. Moreover, TiO_2 is considered a natural semiconductor material that is abundant on Earth, as well as on other planets such as Mars. Therefore,

a perfect correlation between the early atmosphere and the possible origin of O_2 can be formed (Figure 7). The sun, along with TiO_2, could provide continuous conditions for the early atmosphere to produce N_2O and, simultaneously, to decompose N_2O into N_2 and O_2. Accordingly, based on the current evidence outlined above, we conjecture the possible origin of O_2 from the decomposition of N_2O, which could be an important step for the chemical evolution of the early atmosphere to the modern atmosphere.

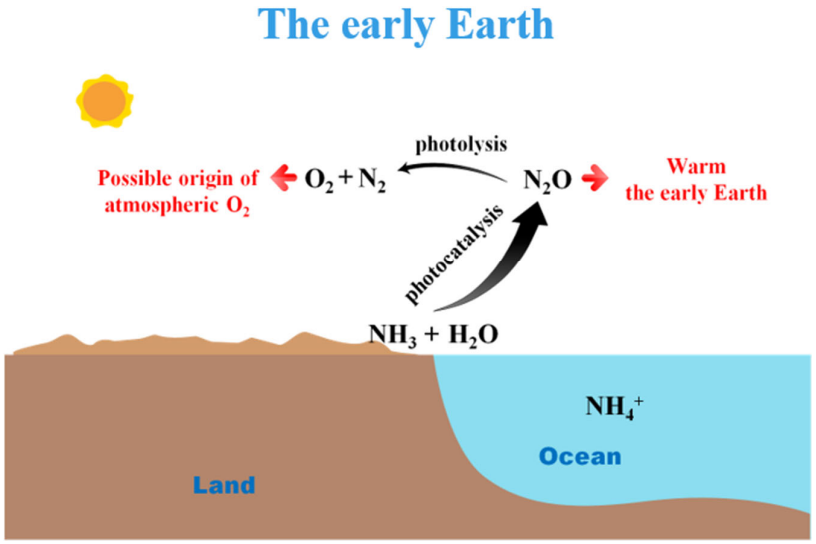

Figure 7. Sketch of the possible primary nitrogen flow on the early Earth.

3. Materials and Methods

3.1. Chemicals

Titanium dioxide (TiO_2, anatase), magnesium sulfate ($MgSO_4$), magnesium chloride ($MgCl_2$), and magnesium bromide ($MgBr_2$) were obtained from Aladin (Shanghai, China). Sodium chloride (NaCl) was supplied by Sinopharm Chemical Reagent Co., Ltd. (Beijing, China). All chemical reagents used in this work were of analytical grade and used as received without further purification or treatment. Pure (99.99%) reaction gases (NH_3, CH_4, N_2O, and H_2) were purchased from Xinghang Gas Co., Ltd. (Fuzhou, China). (and used under the control of flowmeters.

3.2. Characterization

The composition of the gas-phase mixture in the cell was monitored using a Thermo Scientific Nicolet IS50 FT-IR spectrometer (Waltham, MA, USA) equipped with a KBr beam splitter and a DTGS/KBr detector. For each spectrum, 64 scans were accumulated and measured with a resolution of 0.02 cm^{-1} at a range of 1100 to 4000 cm^{-1}. X-ray diffraction data of TiO_2 powder were collected using a Bruker D8 advance X-ray diffractometer (Billerica, MA, USA) (Cu Kα1 irradiation, λ = 1.5406 Å). UV-vis diffuse reflectance spectra were obtained using a Varian Cary 500 UV-Vis-NIR spectrometer with $BaSO_4$ as a reflectance standard (Palo Alto, CA, USA). The morphology of the samples was obtained using a scanning electron microscope (SEM) (JSM-6700F, Tokyo Akishima, Japan) and a TECNAI F30 transmission electron microscope (TEM, Hillsboro, OR, USA). X-ray photoelectron spectroscopy (XPS) analysis of TiO_2 was carried out using monochromatic Al Ka lines and Physical Electrons Quantum 2000 Scanning Esca Microprobe (VG, Madison, WI, USA). The produced N_2O was detected using a gas chromatograph (Agilent 7820A, Santa Clara, CA, USA) equipped with a packed molecular sieve column (CBP-PSN.A) and nitrogen as a carrier gas.

3.3. Photocatalytic Reaction

For the N_2O evolution experiment, a 380 mL (40 cm in long, 3.2 cm in diameter) quartz glass tube equipped with CaF_2 windows was used (Figure S1). TiO_2 (30 mg) was dispersed in 10 mL deionized water or simulated seawater (10 mL, 0.462 M NaCl, 1.3 mM $MgSO_4$, 0.04 M MgCl, 6.8 mM $MgBr_2$) and then poured into the tube. Before light irradiation, the cell was evacuated and refilled with the reaction gas (flow rate, 20 mL/min) several times to remove air inside the tube and finally filled with reaction gas to reach a pressure of one bar. The tube was then sealed and kept at the appropriate reaction temperatures (3 °C or room temperature). The sealed tube was irradiated using a 300 W Xe lamp. The composition of the gas-phase mixture was analyzed using high-resolution Fourier transform infrared spectroscopy (FTIR). In the gas–solid reaction experiment, 30 mg TiO_2 was dispersed in deionized water (5 mL) under ultrasonic stirring. The TiO_2 suspension was then deposited on half of a glass substrate (2 cm × 2 cm), and dried at 60 °C overnight. Finally, the glass substrate was placed into the quartz glass tube with the TiO_2-loaded part of the substrate above the surface of water.

The decomposition of N_2O was performed in the quartz glass tube at room temperature. The reactor was evacuated and purged with N_2 (flow rate, 20 mL/min) several times and finally filled with N_2O (flow rate, 30 mL/min) and N_2 (flow rate, 60 mL/min) to reach a pressure of one bar. The tube was then sealed and irradiated using a 300 W Xe lamp for several days. The composition of the gas-phase mixture was analyzed using gas chromatography [45]. The gas–solid reaction experiments were performed using the same method as above (N_2O evolution experiment), except that the reaction tube was filled with N_2O and N_2.

3.4. Isotope Ratio Mass Spectrometer

The ratio of ^{18}O-labeled H_2O was evaluated using an isotope ratio mass spectrometer (Delta V Advantage, ThermoFisher, Waltham, MA, USA) equipped with an elemental analyzer (FLASH EA 1112) and a ConFlo III versatile interface. The ^{18}O content of the generated N_2O was investigated using a stable isotope ratio mass spectrometer (Mat253, ThermoFisher, Waltham, MA, USA) equipped with a multipurpose online gas preparation instrument (GasBench II, ThermoFisher, Waltham, MA, USA containing a PoraPlotQ chromatographic column (30 m × 0.32 mm) and a GC autosampler (CombiPAL, CTC).

4. Conclusions

In summary, this study revealed a geochemical pathway for the photocatalytic conversion of NH_3 and H_2O to N_2O using a mimicked early reducing atmosphere, providing feasible evidence for the possible transformation of a NH_3-rich atmosphere to a N_2O-rich atmosphere on the early Earth. A N_2O-rich atmosphere would have been more suitable to warm the Earth and provides a favorable way of solving the faint young Sun paradox. Moreover, the photodecomposition of N_2O to N_2 and O_2 may have been an important step in the chemical evolution of the reducing atmosphere to the modern atmosphere. This work offers a possible new insight into the contribution of photocatalysis in the chemical evolution of the early atmosphere, which has crucial implications for understanding the modern Earth system.

Supplementary Materials: The following supporting information can be downloaded at: https://www.mdpi.com/article/10.3390/catal13091310/s1, Figure S1: (a) XRD pattern of TiO_2 and JCPDS standard card (21-1272) [59]; (b) TEM image of TiO_2. (Inset shows the HRTEM of TiO_2, where lattice fringes with a spacing of 0.35 nm correspond to the (101) plane of TiO_2 [60].); Figure S2: (a) UV-Vis diffusion reflectance spectrum (DRS) of TiO_2. (Inset: a value of 3.34 eV was observed read for the band gap of TiO_2 between the $(F(R)hv)^{1/2}$ and E plots.); (b) XPS survey of commercial TiO_2 [61]; (c) Ti 2p lines and fit. The peak at 458.6 eV fits to Ti^{4+}, which is attributed to Ti-O in the TiO_2 [62]; (d) O 1s lines and fit; Figure S3: The production of H_2 and N_2O with TiO_2 and light after 5 days illumination; Figure S4: Comparison of the reaction liquid ion chromatogram after irradiation (black line) and standard ion chromatogram (red line) of NO_3^- and NO_2^-.

Author Contributions: C.H. presented the ideas in the manuscript. C.C. and F.X. conducted experiments. C.C., Q.W. and W.S. analyzed the results. C.C. and F.X. wrote the manuscript with revision from C.H. All authors have read and agreed to the published version of the manuscript.

Funding: This work is supported by the National Natural Science Foundation of China (grant nos. 22072024 and U1662112).

Data Availability Statement: The data that support the findings of this study are available from the corresponding author upon reasonable request.

Conflicts of Interest: The authors declare that they have no conflict of interest.

References

1. Goldblatt, C.; Zahnle, K.J. Faint young Sun paradox remains. *Nature* **2011**, *474*, E1. [CrossRef]
2. Sagan, C.; Mullen, G. Earth and Mars: Evolution of atmospheres and surface temperatures. *Science* **1972**, *177*, 52–56. [CrossRef]
3. Peck, W.H.; Valley, J.W.; Wilde, S.A.; Graham, C.M. Oxygen isotope ratios and rare earth elements in 3.3 to 4.4 Ga zircons: Ion microprobe evidence for high delta O^{18} continental crust and oceans in the Early Archean. *Geochim. Cosmochim. Acta* **2001**, *65*, 4215–4229. [CrossRef]
4. Kiehl, J.T.; Dickinson, R.E. A Study of the Radiative Effects of Enhanced Atmospheric CO_2 and CH_4 on Early Earth Surface Temperatures. *J. Geophys. Res. Atmos.* **1987**, *92*, 2991–2998. [CrossRef]
5. Byrne, B.; Goldblatt, C. Diminished greenhouse warming from Archean methane due to solar absorption lines. *Clim. Past* **2015**, *11*, 559–570. [CrossRef]
6. Rosing, M.T.; Bird, D.K.; Sleep, N.H.; Bjerrum, C.J. No climate paradox under the faint early Sun. *Nature* **2010**, *464*, 744–747. [CrossRef]
7. Airapetian, V.S.; Glocer, A.; Gronoff, G.; Hébrard, E.; Danchi, W. Prebiotic chemistry and atmospheric warming of early Earth by an active young Sun. *Nat. Geosci.* **2016**, *9*, 452–455. [CrossRef]
8. Lan, X.; Zhu, L.; Yuan, Q. Long-Term Variation of Greenhouse Gas N_2O Observed by MLS during 2005–2020. *Remote Sens.* **2022**, *14*, 955. [CrossRef]
9. Rotmans, J.; Elzen, M.G.J.D. A model-based approach to the calculation of global warming potentials (GWP). *Int. J. Clim.* **1992**, *12*, 865–874. [CrossRef]
10. Nna-Mvondo, D.; Navarro-González, R.; Raulin, F.; Coll, P. Nitrogen Fixation By Corona Discharge On The Early Precambrian Earth. *Space Life Sci.* **2005**, *35*, 401–409. [CrossRef]
11. Paytan, A. Earth history—Sulfate clues for the early history of atmospheric oxygen. *Science* **2000**, *288*, 626–627. [CrossRef]
12. Planavsky, N.J.; Asael, D.; Hofmann, A.; Reinhard, C.T.; Lalonde, S.V.; Knudsen, A.; Wang, X.L.; Ossa, F.O.; Pecoits, E.; Smith, A.J.B.; et al. Rouxel Evidence for oxygenic photosynthesis half a billiion years before the Great Oxidation Event. *Nat. Geosci.* **2014**, *7*, 283–286. [CrossRef]
13. Sumner, D.Y.; Hawes, I.; Mackey, T.J.; Jungblut, A.D.; Doran, P.T. Antarctic microbial mats: A modern analog for Archean lacustrine oxygen oases. *Geology* **2015**, *43*, 887–890. [CrossRef]
14. Olson, S.L.; Kump, L.R.; Kasting, J.F. Quantifying the areal extent and dissolved oxygen concentrations of Archean oxygen oases. *Chem. Geol.* **2013**, *362*, 35–43. [CrossRef]
15. Dismukes, G.C.; Klimov, V.V.; Baranov, S.V.; Kozlov, Y.N.; DasGupta, J.; Tyryshkin, A. The origin of atmospheric oxygen on Earth: The innovation of oxygenic photosynthesis. *Proc. Natl. Acad. Sci. USA* **2001**, *98*, 2170–2175. [CrossRef]
16. Lu, Z.; Chang, Y.C.; Yin, Q.-Z.; Ng, C.Y.; Jackson, W.M. Evidence for direct molecular oxygen production in CO_2 photodissociation. *Science* **2014**, *346*, 61–64. [CrossRef]
17. Wang, X.D.; Gao, X.F.; Xuan, C.J.; Tian, S.X. Dissociative electron attachment to CO_2 produces molecular oxygen. *Nat. Chem.* **2016**, *8*, 258–263. [CrossRef]
18. Yamashita, T.A. Vannice N_2O decomposition over manganese oxides. *J. Catal.* **1996**, *161*, 254–262. [CrossRef]
19. Tsuji, M.; Kawahara, M.; Noda, K.; Senda, M.; Sako, H.; Kamo, N.; Kawahara, T.; Kamarudin, K.S. Photochemical removal of NO_2 by using 172-nm Xe_2 excimer lamp in N_2 or air at atmospheric pressure. *J. Hazard. Mater.* **2009**, *162*, 1025–1033. [CrossRef] [PubMed]
20. Yuan, D.; Yu, S.; Xie, T.; Chen, W.; Wang, S.; Tan, Y.; Wang, T.; Yuan, K.; Yang, X.; Wang, X. Photodissociation Dynamics of Nitrous Oxide near 145 nm: The O(1S0) and O(3PJ=2,1,0) Product Channels. *J. Phys. Chem. A* **2018**, *122*, 2663–2669. [CrossRef] [PubMed]
21. Honma, K. Laser initiated reactions in N_2O clusters studied by time-sliced ion velocity imaging technique. *J. Chem. Phys.* **2013**, *139*, 044307. [CrossRef] [PubMed]
22. McCollom, T.M. Miller-Urey and Beyond: What Have We Learned About Prebiotic Organic Synthesis Reactions in the Past 60 Years? *Annu. Rev. Earth Planet. Sci.* **2013**, *41*, 207–229. [CrossRef]
23. Ning, S.; Ou, H.; Li, Y.; Lv, C.; Wang, S.; Wang, D.; Ye, J. $Co^0-Co^{\delta+}$ Interface Double-Site-Mediated C-C Coupling for the Photothermal Conversion of CO_2 into Light Olefins. *Angew. Chem. Int. Ed.* **2023**, *62*, e202302253. [CrossRef]

24. Ning, S.; Xu, H.; Qi, Y.; Song, L.; Zhang, Q.; Ouyang, S.; Ye, J. Microstructure Induced Thermodynamic and Kinetic Modulation to Enhance CO_2 Photothermal Reduction: A Case of Atomic-Scale Dispersed Co-N Species Anchored Co@C Hybrid. *ACS Catal.* **2020**, *10*, 4726–4736. [CrossRef]
25. Ning, S.; Sun, Y.; Ouyang, S.; Qi, Y.; Ye, J. Solar light-induced injection of hot electrons and photocarriers for synergistically enhanced photothermocatalysis over Cu-Co/$SrTiO_3$ catalyst towards boosting CO hydrogenation into C2–C4 hydrocarbons. *Appl. Catal. B Environ.* **2022**, *310*, 121063. [CrossRef]
26. Cnossen, I.; Sanz-Forcada, J.; Favata, F.; Witasse, O.; Zegers, T.; Arnold, N.F. Habitat of early life: Solar X-ray and UV radiation at Earth's surface 4–3.5 billion years ago. *J. Geophys. Res.* **2007**, *112*, E02008. [CrossRef]
27. Cockell, C.S. The ultraviolet history of the terrestrial planets—implications for biological evolution. *Planet. Space Sci.* **2000**, *48*, 203–214. [CrossRef]
28. Avice, G.; Marty, B.; Burgess, R. The origin and degassing history of the Earth's atmosphere revealed by Archean xenon. *Nat. Commun.* **2017**, *8*, 15455. [CrossRef] [PubMed]
29. Reiche, H.; Bard, A.J. Heterogeneous photosynthetic production of amino acids from methane-ammonia-water at platinum/titanium dioxide. implications in chemical evolution. *Chem. Informationsdienst* **1979**, *10*, 3127–3128. [CrossRef]
30. Doane, T.A. A survey of photogeochemistry. *Geochem. Trans.* **2017**, *18*, 1. [PubMed]
31. Ferris, J.P.; Hill, A.R.; Liu, R.H.; Orgel, L.E. Synthesis of long prebiotic oligomers on mineral surfaces. *Nature* **1996**, *381*, 59–61. [CrossRef]
32. Hazen, R.M.; Papineau, D.; Leeker, W.B.; Downs, R.T.; Ferry, J.M.; McCoy, T.J.; Sverjensky, D.A.; Yang, H.X. Mineral evolution. *Am. Mineral.* **2008**, *93*, 1693–1720. [CrossRef]
33. Byrne, B.; Goldblatt, C. Radiative forcings for 28 potential Archean greenhouse gases. *Clim. Past.* **2014**, *10*, 2011–2053. [CrossRef]
34. Chyba, C.F. Atmospheric science—Rethinking Earth's early atmosphere. *Science* **2005**, *308*, 962–963. [CrossRef] [PubMed]
35. Ore, C.M.D.; Cruikshank, D.P.; Protopapa, S.; Scipioni, F.; McKinnon, W.B.; Cook, J.C.; Grundy, W.M.; Schmitt, B.; Stern, S.A.; Moore, J.M.; et al. Detection of ammonia on Pluto's surface in a region of geologically recent tectonism. *Sci. Adv.* **2019**, *5*, eaav5731. [CrossRef]
36. Healy, M.G.; Ibrahim, T.G.; Lanigan, G.J.; Serrenho, A.J.; Fenton, O. Nitrate removal rate, efficiency and pollution swapping potential of different organic carbon media in laboratory denitrification bioreactors. *Ecol. Eng.* **2012**, *40*, 198–209. [CrossRef]
37. Stüeken, E.E.; Kipp, M.A.; Koehler, M.C.; Buick, R. The evolution of Earth's biogeochemical nitrogen cycle. *Earth-Sci. Rev.* **2016**, *160*, 220–239. [CrossRef]
38. Stueken, E.E. Nitrogen in Ancient Mud: A Biosignature? *Astrobiology* **2016**, *16*, 730–735. [CrossRef]
39. Stüeken, E.; Buick, R.; Schauer, A. Nitrogen isotope evidence for alkaline lakes on late Archean continents. *Earth Planet. Sci. Lett.* **2015**, *411*, 1–10. [CrossRef]
40. Rapf, R.J.; Vaida, V. Sunlight as an energetic driver in the synthesis of molecules necessary for life. *Phys. Chem* **2016**, *18*, 20067–20084. [CrossRef]
41. Buick, R. Did the Proterozoic 'Canfield Ocean' cause a laughing gas greenhouse? *Geobiology* **2010**, *5*, 97–100. [CrossRef]
42. Roberson, A.L.; Roadt, J.; Halevy, I.; Kasting, J.F. Greenhouse warming by nitrous oxide and methane in the Proterozoic Eon. *Geobiology* **2011**, *9*, 313–320. [CrossRef] [PubMed]
43. Miller, S.L. A Production of Amino Acids Under Possible Primitive Earth Conditions. *Science* **1953**, *117*, 528–529. [CrossRef] [PubMed]
44. Ferus, M.; Pietrucci, F.; Saitta, A.M.; Knížek, A.; Kubelík, P.; Ivanek, O.; Shestivska, V.; Civiš, S. Formation of nucleobases in a Miller–Urey reducing atmosphere. *Proc. Natl. Acad. Sci. USA* **2017**, *114*, 4306–4311. [CrossRef]
45. Liu, Y.M.; Cheng, Z.; He, B.; Gu, C.; Xiao, T.; Zhou, Z.; Guo, J.; Liu, H.; He, B.; Ye, B.; et al. Pothole-rich ultrathin WO_3 nanosheets triggering N≡N bond activation of nitrogen for direct nitrate photosynthesis. *Angew. Chem. Int. Ed.* **2018**, *58*, 731–735. [CrossRef]
46. Plank, T.; Langmuir, C.H. The chemical composition of subducting sediment and its consequences for the crust and mantle. *Chem. Geol.* **1998**, *145*, 325–394. [CrossRef]
47. Civiš, S.; Knížek, A.; Ivanek, O.; Kubelík, P.; Zukalová, M.; Kavan, L.; Ferus, M. The origin of methane and biomolecules from a CO_2 cycle on terrestrial planets. *Nat. Astron.* **2017**, *1*, 721–726. [CrossRef]
48. Montzka, S.A.; Dlugokencky, E.J.; Butler, J.H. Non-CO_2 greenhouse gases and climate change. *Nature* **2011**, *476*, 43–50. [CrossRef]
49. Riding, R.; Fralick, P.; Liang, L. Identification of an Archean marine oxygen oasis. *Precambrian Res.* **2014**, *251*, 232–237. [CrossRef]
50. Mloszewska, A.M.; Cole, D.B.; Planavsky, N.J.; Kappler, A.; Whitford, D.S.; Owttrim, G.W.; Konhauser, K.O. UV radiation limited the expansion of cyanobacteria in early marine photic environments. *Nat. Commun.* **2018**, *9*, 3088. [CrossRef]
51. Sheridan, P.P.; Freeman, K.H.; Brenchley, J.E. Estimated minimal divergence times of the major bacterial and archaeal phyla. *Geomicrobiol. J.* **2003**, *20*, 1–14. [CrossRef]
52. Komiya, T.; Hirata, T.; Kitajima, K.; Yamamoto, S.; Shibuya, T.; Sawaki, Y.; Ishikawa, T.; Shu, D.; Li, Y.; Han, J. Evolution of the composition of seawater through geologic time, and its influence on the evolution of life. *Gondwana Res.* **2008**, *14*, 159–174. [CrossRef]
53. Och, L.M.; Shields-Zhou, G.A. The Neoproterozoic oxygenation event: Environmental perturbations and biogeochemical cycling. *Earth Sci. Rev.* **2012**, *110*, 26–57. [CrossRef]
54. Kannan, S.; Swamy, C.S. Catalytic Decomposition of Nitrous-Oxide on in-Situ Generated Thermally Calcined Hydrotalcites. *Appl. Catal. B* **1994**, *3*, 109–116. [CrossRef]

55. Johnston, D.; Poulton, S.; Goldberg, T.; Sergeev, V.; Podkovyrov, V.; Vorob'Eva, N.; Bekker, A.; Knoll, A. Late Ediacaran redox stability and metazoan evolution. *Earth Planet. Sci. Lett.* **2012**, *335–336*, 25–35. [CrossRef]
56. Selwyn, G.S.; Johnston, H.S. Ultraviolet absorption spectrum of nitrous oxide as a function of temperature and isotopic substitution. *J. Chem. Phys.* **1981**, *74*, 3791–3803. [CrossRef]
57. Harding, D.J.; Neugebohren, J.; Grütter, M.; Schmidt-May, A.F.; Auerbach, D.J.; Kitsopoulos, T.N.; Wodtke, A.M. Single-field slice-imaging with a movable repeller: Photodissociation of N_2O from a hot nozzle. *J. Chem. Phys.* **2014**, *141*, 054201. [CrossRef]
58. Angulo-Brown, F.; Rosales, M.A.; Barranco-Jiménez, M.A. The Faint Young Sun Paradox: A Simplified Thermodynamic Approach. *Adv. Astron.* **2012**, *2012*, 478957. [CrossRef]
59. Yang, H.G.; Sun, C.H.; Qiao, S.Z.; Zou, J.; Liu, G.; Smith, S.C.; Cheng, H.M.; Lu, G.Q. Anatase TiO_2 single crystals with a large percentage of reactive facets. *Nature* **2008**, *453*, 638–641. [CrossRef] [PubMed]
60. Wang, W.K.; Chen, J.J.; Zhang, X.; Huang, Y.X.; Li, W.W.; Yu, H.Q. Self-induced synthesis of phase-junction TiO_2 with a tailored rutile to anatase ratio below phase transition temperature. *Sci. Rep.* **2016**, *6*, 20491. [CrossRef]
61. Yu, Y.; Wen, W.; Qian, X.Y.; Liu, J.B.; Wu, J.M. UV and visible light photocatalytic activity of Au/TiO_2 nanoforests with Anatase/Rutile phase junctions and controlled Au locations. *Sci. Rep.* **2017**, *7*, 41253. [CrossRef] [PubMed]
62. Batalovic, K.; Bundaleski, N.; Radakovic, J.; Abazovic, N.; Mitric, M.; Silva, R.A.; Savic, M.; Belosevic-Cavor, J.; Rakocevic, Z.; Rangel, C.M. Modification of N-doped TiO_2 photocatalysts using noble metals (Pt, Pd)—A combined XPS and DFT study. *Phys. Chem. Chem. Phys.* **2017**, *19*, 7062–7071. [CrossRef] [PubMed]